JOURNAL OF VIROLOGY, Jan. 1989, p. 94–100
0022-538X/89/010094-07$02.00/0

Vol. 63, No. 1

The Zinc Finger Region of Simian Virus 40 Large T Antigen

GERHARD LOEBER, RAMON PARSONS, AND PETER TEGTMEYER*

Department of Microbiology, State University of New York, Stony Brook, New York 11794

Received 11 July 1988/Accepted 27 September 1988

Simian virus 40 large T antigen contains a single sequence element with an arrangement of cysteines and histidines that is characteristic of a zinc finger motif. The finger region maps from amino acids 302 through 320 and has the sequence Cys-302LeuLysCys-305IleLysLysGluGlnProSerHisTyrLysTyrHis-317GluLysHis-320. In a conventional representation, the binding of zinc to the cysteines and histidines at positions 302, 305, 317, and 320 would form two minor loops and one major loop from the intervening amino acids. We made single amino acid substitutions at every position in the finger to identify possible functional elements within the putative metal-binding domain. Amino acids in the zinc finger could be divided into three classes characterized by distinct roles in DNA replication and transformation. Class 1 consisted of amino acids in the two minor loops of the finger and in the amino-terminal part of the major loop. Mutations here did not affect either replication or transformation. Class 2 consisted of the SerHisTyrLysTyr amino acids located in the carboxy terminus of the major loop of the finger. Mutations in this contiguous region reduced replication of the mutant viruses to different degrees. This clustering suggested that the region is an active site important for a specific function in DNA replication. With the exception of a mutation in the histidine at position 313, these mutations had no effect on transformation. Class 3 consisted of the proposed zinc-binding amino acids at positions 302, 305, 317, and 320 and the histidine at position 313 in the major loop of the finger. Mutations in these amino acids abolished the viability of the virus completely and had a distinctive effect on the transforming functions of the protein. Thus, the five cysteines and histidines of class 3 may play an important role in determining the overall structure of the protein. The histidine at position 313 may function both in the active site where it is located and in cooperation with the proposed zinc-binding ligands.

Simian virus 40 (SV40) large T antigen is the major regulatory protein in the SV40 life cycle and serves as an attractive model for many functions in molecular biology. During productive infection of permissive cells, T antigen performs a number of related functions in viral DNA replication. After binding to the origin of replication (12, 48), T antigen initiates DNA replication by denaturing origin duplex DNA (10, 52) and perhaps by guiding cellular proteins such as DNA polymerase alpha (40) to the origin replication bubble. The helicase activity of T antigen (42, 43, 51) then moves the replication forks around the circular DNA as a prerequisite for the elongation of daughter strands. At the time of the onset of viral DNA replication, T antigen coordinates viral transcription with DNA replication by repressing early transcription (34, 46) and inducing late transcription (4, 8). In nonpermissive cells, T antigen induces and maintains the transformed state by unknown mechanisms (50). T-antigen induction of cellular transcription (24) and of DNA synthesis (5) and the interaction of T antigen with cellular protein p53 (17, 27) play additional roles in productive and transforming infections.

The related functions of SV40 large T antigen may be coordinated by the organization of distinct functional domains in the protein. Perhaps the best-characterized domain is the origin-binding domain. The region responsible for minimal specific binding to the origin of DNA replication is located between amino acids (AAs) 131 and 257 (32, 39, 44). A small region with an amino acid sequence very similar to those of known nucleotide-binding sites maps between AAs 418 and 528; presumably, this region is related to the intrinsic ATPase activity of T antigen (3, 49). Other domains have been mapped less precisely. For example, the helicase domain is located between residues 131 and 680, but its precise limits are not known (42, 51). The residues responsible for the binding of T antigen to DNA polymerase alpha and p53 are located somewhere between positions 272 and 517 (17, 37, 40). SV40 T antigen contains a single sequence element with an arrangement of cysteines and histidines that is characteristic of a zinc finger motif (25). This putative metal-binding domain maps from AAs 302 through 320 and falls within many of the functional domains of T antigen. It is located outside the minimal origin-binding region but is still within the protein fragment (AAs 131 through 371) required for optimal binding to the origin sequences (39).

Zinc finger motifs are common in a wide variety of procaryotic and eucaryotic proteins. In many cases, the fingers appear to contribute to DNA recognition and binding. Examples of this class of protein include transcription factor IIIA (31), transcription factor Sp-1 (22) and, most probably, proteins encoded by developmentally regulated genes (6, 35). Proteins in this class have multiple repeats of a finger domain with a characteristic arrangement of two cysteines and histidines which coordinate the metal ion. These proteins also contain two aromatic residues and one leucine at distinctive positions within the finger. Klug and Rhodes (25) have proposed that the major loop of the zinc finger comes into close and specific contact with the major groove of DNA. SV40 T antigen has a single finger motif that has two aromatic amino acids, but these are not located in positions characteristic of a classical DNA-binding finger. However, metal fingers need not be multiple, may have a variety of alternative sequences, and may have important functions other than the direct binding of protein to specific DNA sequences (2, 15). Examples of proteins with alternative finger structures include the T4 gene 32 protein (18), the sigma-3 protein of reovirus (36), and the E1A protein of adenovirus (28). Berg (2) and Frankel and Pabo (15) have

* Corresponding author.

proposed that metal-binding domains contribute to protein-protein interactions or determine overall protein structure.

In the T antigens encoded by all known polyomaviruses, a zinc finger motif is highly conserved (16, 33, 50). This finding implies that the sequence element plays an important role in T-antigen function. We have undertaken a systematic mutational analysis of the zinc finger in SV40 T antigen by making specific single AA exchanges at every position of the finger sequence. Functional analysis of the mutants in lytic and transforming infections has allowed us to identify three characteristic phenotypes in this region. Using in vivo replication assays, we were able to relate the zinc finger to a function involved in DNA replication.

MATERIALS AND METHODS

Cells and bacterial strains. *Escherichia coli* BMH71-18 and M13 helper phage K07 were obtained from International Biotechnologies, Inc. (New Haven, Conn.). *E. coli* BW313 was kindly provided by B. Bachmann. This strain is defective in two genes involved in DNA metabolism (*dut* and *ung*) and randomly incorporates uracil instead of thymidine into DNA (14). Primary mouse embryo fibroblast (MEF) cells were prepared from 11- to 14-day-old C57BL/6 mouse embryos (47).

Construction of pBS-SV40. To construct pBS-SV40, SV40 strain 776 DNA was cleaved with *Bam*HI, cloned into the *Bam*HI site of the Bluescript-SK(+) vector (Stratagene, La Jolla, Calif.), and grown in *E. coli* BMH71-18. The Bluescript-SK(+) vector contains an M13 origin as well as a plasmid (ColE1) origin. Thus, DNA could be isolated either in single-stranded form for use as a target for mutagenesis or in double-stranded form for functional studies.

Preparation of single-stranded, uracil-containing pBS-SV40 DNA. *E. coli* BMH71-18 cells carrying plasmid pBS-SV40 were superinfected with the M13 helper phage K07. Phage particles containing single-stranded pBS-SV40 DNA were used to infect *E. coli* BW313 (26). Ampicillin-resistant colonies of BW313 were selected on LB plates containing 100 μg of ampicillin, 100 μg of deoxyadenosine, and 20 μg of thymidine per ml. To obtain single-stranded, uracil-containing pBS-SV40 DNA, we inoculated single colonies of BW313(pBS-SV40) into 100 ml of LB containing 100 μg of ampicillin per ml, 0.25 μg of uridine per ml, and 100 μl of an M13 helper phage K07 stock (>10^{10} PFU/ml) and grew them overnight. After centrifugation, the single-stranded DNA was isolated from the supernatant as described by J. Messing (30) and purified by alkaline sucrose gradient centrifugation.

Construction of the zinc finger mutants. The zinc finger sequence of SV40 large T antigen is located between amino acids 302 and 320, encoded by bases 3858 through 3914 in the viral genome (50). Mutants with base substitutions in this region of the viral genome were constructed by oligonucleotide-directed mutagenesis with uracil-containing single-stranded DNA as a template. The oligonucleotides were 16 to 22 bases long and had one base mismatch that would encode a single amino acid substitution in the T-antigen gene. Typically, 10 to 20 ng of phosphorylated oligonucleotide was annealed to 100 ng of uracil-containing template. The second strand was synthesized in the presence of all four deoxynucleotides with T4 DNA polymerase in a total reaction volume of 20 μl. The remaining nick in the double-stranded DNA was sealed with T4 DNA ligase. The mutated DNA (0.5 μl) was transfected into *E. coli* BMH71-18, and ampicillin-resistant colonies were selected and grown to isolate DNA. After DNA extraction, the clones were sequenced without preliminary screening to identify mutants. Depending on the oligonucleotide used, 50 to 90% of the sequenced clones contained the desired mutation.

Plaque assay. For the plaque assay, 10 μg of CsCl-purified mutant DNA was cleaved with *Bam*HI and religated with T4 DNA polymerase in a total reaction volume of 600 μl. Agarose gel electrophoresis showed that about 5% of the religated DNA was single-copy, covalently closed SV40 DNA; the rest was multimeric forms of vector and virus DNAs. Either 4 or 40 ng of total religated DNA was transfected into confluent CV-1 cells with DEAE-dextran (29), and the cultures were maintained under agar containing Dulbecco modified Eagle medium with 10% fetal calf serum for 4 to 7 weeks. Plaques were visualized by staining with neutral red (45).

Transformation assay. For transformation assays, 10^5 primary MEF cells were seeded in 75-cm^2 flasks. Cells were transfected with mutant DNAs (1 to 5 μg per flask plus 5 to 9 μg of carrier DNA) by the calcium phosphate procedure (20) and were fed twice a week with Dulbecco modified Eagle medium containing 10% fetal calf serum. Foci were scored 3 to 5 weeks after the transfection.

DNA replication in vivo. The viral DNA replication of the mutants was measured in CV-1 cells. Mutant DNA (3.0 μg) was transfected into a 75-cm^2 flask of subconfluent CV-1 cells with DEAE-dextran (29). Viral DNA was extracted 72 h after transfection (21) and digested with *Mbo*I. Replicated DNA was assayed as described previously (11).

RESULTS

Choice of the amino acid substitution mutants. To compare the importance of various amino acid positions and to identify possible functional regions in the zinc finger region, we introduced amino acid exchanges of similar severity in each position. As a guideline for the selection of the appropriate exchanges, we used the amino acid score matrix of Staden (41). This matrix is derived from the protein atlas of Dayhoff (9) and is based on a comparison of the primary sequences of many families of functionally related proteins. The matrix establishes an evolutionary hierarchy of the functional interchangeability of various amino acids. Table 1 shows the positions of the changes introduced into the viral genome and the resulting changes in the amino acid sequence of T antigen. Except for some special positions, the alterations in the protein were of intermediate severity.

Viral replication of the zinc finger mutants. After mutagenesis, viral DNAs were excised from bacterial plasmids and religated as described in Materials and Methods. We used the viral DNA to test the ability of the mutants to induce plaques in a monolayer of permissive CV-1 cells. Under our conditions, 1 ng of wild-type (WT) DNA produced approximately 200 plaques. The histogram in Fig. 1A shows a summary of the results of these plaque assays for WT and mutant DNAs. We divided the mutants into three classes based on their ability to grow in CV-1 cells.

The first class consisted of mutants with mutations which affected positions in the minor loops of the finger (AAs 303, 304, 318, and 319) and positions in the amino-terminal part of the major loop (AAs 306 through 311). These mutants (Fig. 1A, open bars) induced plaques with a WT morphology and at a WT frequency. The minor differences in the numbers of plaques were consistent with the experimental error inherent in the transfection technique.

The second class consisted of mutants with mutations clustered in the carboxy-terminal part of the major loop

TABLE 1. Sequence alterations in the zinc finger region of SV40 T antigen

Mutant	Position	Codon change	Amino acid change
302-S	3913	TGT to TCT	Cys to Ser
303-F	3909	TTA to TTT	Leu to Phe
304-R	3907	AAA to AGA	Lys to Arg
305-S	3904	TGT to TCT	Cys to Ser
306-T	3901	ATT to ACT	Ile to Thr
307-N	3897	AAA to AAC	Lys to Asn
308-E	3896	AAA to GAA	Lys to Glu
309-G	3892	GAA to GGA	Glu to Gly
310-P	3889	CAG to CCG	Gln to Pro
311-R	3886	CCC to CGC	Pro to Arg
312-I	3883	AGC to ATC	Ser to Ile
313-L	3880	CAC to CTC	His to Leu
313-R	3880	CAC to CGC	His to Arg
314-S	3877	TAT to TCT	Tyr to Ser
315-E	3875	AAG to GAG	Lys to Glu
315-R	3874	AAG to AGG	Lys to Arg
316-N	3872	TAC to AAC	Tyr to Asn
317-Q	3867	CAT to CAG	His to Gln
318-V	3865	GAA to GTA	Glu to Val
319-N	3861	AAG to AAC	Lys to Asn
320-L	3859	CAT to CTT	His to Leu

(AAs 312 through 316). The numbers of plaques induced by these mutants (Fig. 1A, shaded bars) were only slightly lower than the numbers of WT plaques in most cases, but the plaques were slow to appear and small (Fig. 1B). The reduction in size was slight for mutant 316-N and moderate for mutants 312-I and 314-S. Mutant 315-E produced less than 10% of the WT number of plaques; these first appeared about 4 weeks after transfection and did not grow to more than pinpoint size. Since the lysine-to-glutamic acid mutation altered the charge at position 315, a lysine-to-arginine mutation was also constructed. The resulting mutant was able to replicate at WT levels and induce plaques of WT size. Thus, the reduced replication of mutant 315-E was due to a charge effect. Mutant 313-L failed to make any plaques even after incubation for 8 weeks.

The third class consisted of mutants 302-S, 305-S, 317-Q, 320-L, and 313-L. The first four mutations affected cysteines and histidines arranged in positions characteristic of zinc-binding amino acids. The remaining mutation changed a histidine in the major loop of the putative finger. These mutants failed to replicate at all; no cytopathic effects in the CV-1 cells could be detected even after incubation for 40 days. Another mutant, 313-R, which maintained the positive charge of the histidine in the WT T antigen at position 313 by changing it to an arginine, was equally unable to replicate. This result suggests that a histidine is important at that position. The inability of class 3 mutants to grow was not due to second site mutations in the late region of the genome, since all replication-negative mutants were able to induce cytopathic effects in COS-1 cells (19), which express WT T antigen constitutively. Second site mutations in T antigen were also highly unlikely, because multiple independent clones of each defective mutant had identical phenotypes.

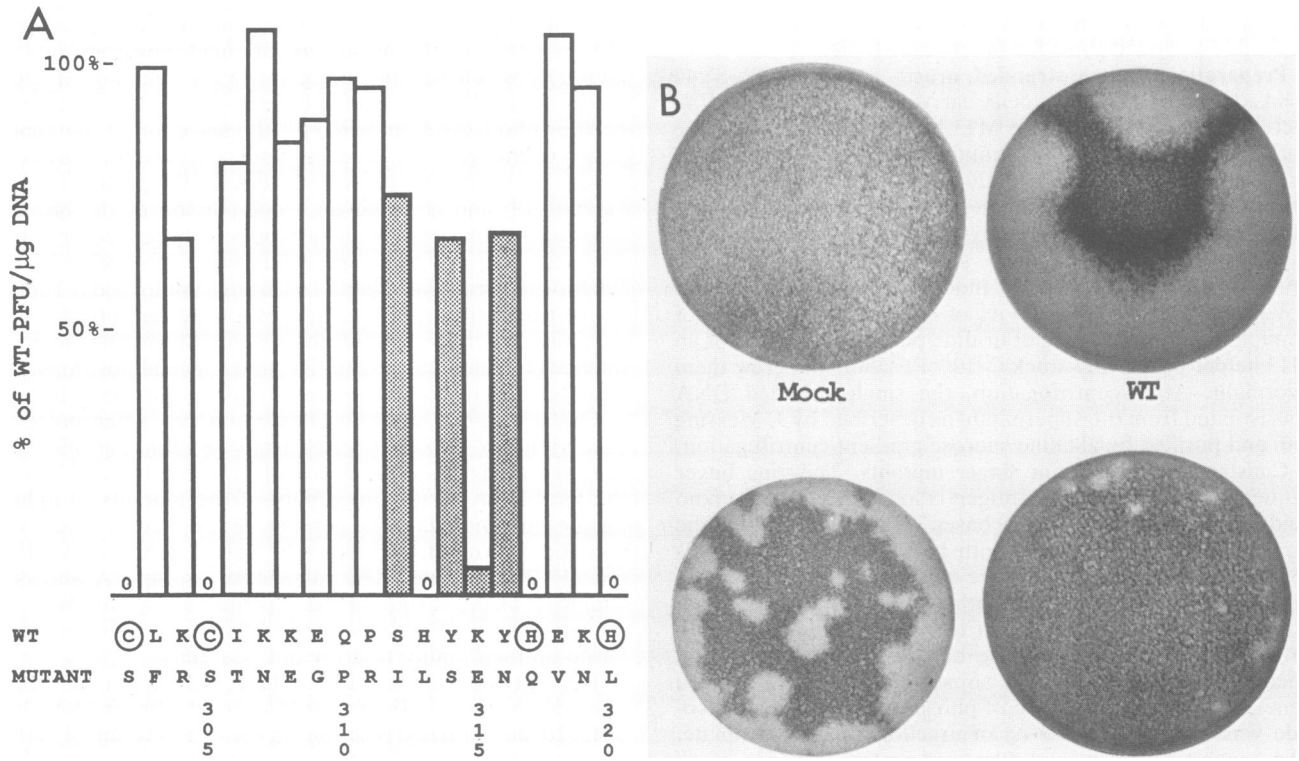

FIG. 1. Plaque formation by WT and mutant viruses. (A) Bar histogram of the efficiency of plaque formation by WT and mutant DNAs. WT amino acid positions and the single amino acid substitutions in the mutant DNAs are shown in the single-letter code at the bottom of the histogram; the corresponding positions in the protein are shown below. Putative zinc-binding amino acids are circled. The height of the columns compares the number of plaques induced by mutant DNA with the number of plaques induced by WT DNA under identical conditions. Open bars indicate large plaques, shaded bars indicate small plaques, and zeros in bars indicate no plaques. (B) Representative plaques produced by WT and mutant DNAs. CV-1 cells were infected as described in Materials and Methods. The plates shown were incubated at 37°C for 35 days. The WT sample was diluted 10-fold for comparison of plaque morphology.

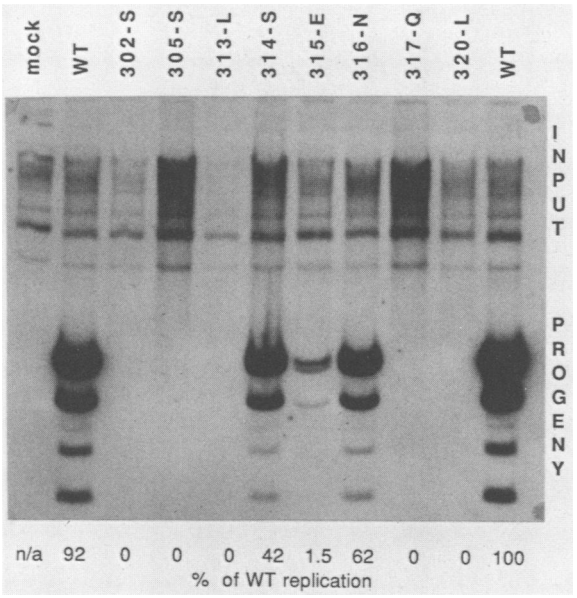

FIG. 2. DNA replication of mutants in CV-1 cells. The mutants are identified at the top of the figure. The replication efficiency of each mutant DNA was determined by transfection of subconfluent CV-1 cells, extraction of DNA (21) after 72 h, *Mbo*I digestion, and Southern blot analysis. The efficiency of replication, quantitated by densitometric scanning of the replicated bands, is shown at the bottom of the figure. mock, Transfection of cells with the Bluescript-SK(+) plasmid that contains no insertion of SV40 DNA; n/a, not applicable.

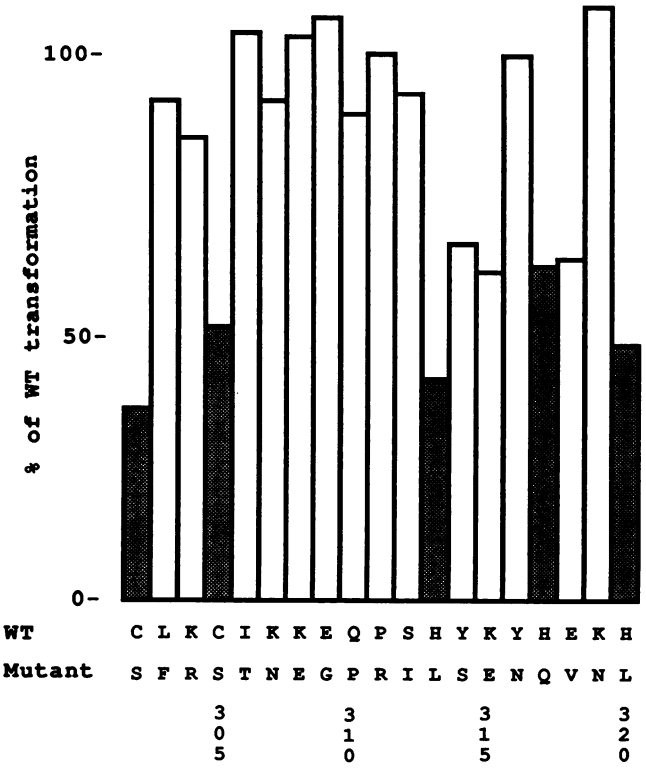

FIG. 3. Transformation of primary mouse cells. The diagram shows the number of foci induced by mutants after DNA transfection of primary MEF cells. WT and mutant amino acids are shown in the single-letter code; the corresponding positions in the protein are shown below. The height of the columns compares the number of foci induced by mutant DNA with those induced by WT SV40 DNA. Open bars indicate large and small colonies, and shaded bars indicate small colonies only.

DNA replication in vivo. The results of the plaque assays identified mutants with little or no ability to grow in CV-1 cells. To localize these defects, which could either be involved directly in DNA replication or affect other functions in the growth cycle, we transfected mutant DNA into CV-1 cells and extracted episomal DNA after 72 h. We used *Mbo*I to discriminate methylated input DNA from unmethylated replicated DNA (11). Figure 2 shows the results of the in vivo replication experiments for mutant 302-S, 305-S, 313-L, 314-S, 315-E, 316-N, 317-Q, and 320-L DNAs and WT SV40 DNA. As quantitated by densitometric scanning of the replicated bands, the replication efficiency was 62% of the WT for 316-N, 42% of the WT for 314-S, and less than 2% of the WT for 315-E. These data correlate well with the reduced growth rate observed in the plaque assays. No replicated bands, even after prolonged exposure of the autoradiograph, could be detected for mutants 302-S, 305-S, 313-L, 317-Q, and 320-L. Thus, the defect in viral growth could be localized to a function prior to or during DNA replication.

Transformation of nonpermissive cells. The ability of the zinc finger mutants to transform primary MEF cells was tested in a focus formation assay. Figure 3 summarizes the results of these experiments. The mutants fell into two classes based on their ability to form transformed foci on primary MEF cells.

The first class (Fig. 3, open bars) consisted of all mutants which were able to replicate, including mutant 315-E, which replicated only at a very reduced rate. These mutants induced transformed foci on primary MEF cells with a WT efficiency (50 to 100 foci per flask, depending on the experiment). The foci also had WT size and morphology. Minor differences in the number of foci were considered to be insignificant, since the ability of duplicate samples of WT DNA to transform cells varied to a similar extent. Such variations in transformation assays have been noted in other studies (23, 38). Foci induced by these mutants were cloned and expanded to stable transformed cell lines. All transformed clones expressed T antigen, as determined by immunofluorescent-antibody staining (data not shown). A small decrease in the efficiency of transformation by the first class of mutants could not be excluded because the transformation assay was performed beyond the linear range of transformation per microgram of DNA (data not shown) (47).

The second class (Fig. 3, shaded bars) consisted of mutants with mutations which affected the presumed zinc-binding amino acids and mutations at position 313. This class was identical to the class which completely failed to replicate in permissive cells. The mutants were able to transform primary MEF cells, but the number of foci induced was slightly lower than the number of foci induced by WT SV40 DNA. Furthermore, foci induced by these mutants were significantly smaller and appeared later after transfection. Figure 4 shows the morphology of foci induced by WT SV40 DNA, by the minute-plaque-mutant 315-E, and by mutants 302-S and 313-L. Although not shown here, mutants 305-S, 313-R, 317-Q, and 320-L induced the same small foci as did mutants 302-S and 313-L. Immunofluorescent-antibody staining showed that these small foci were positive for T-antigen expression. It was difficult to establish cell lines from the small transformed foci. Less than 5% of the foci

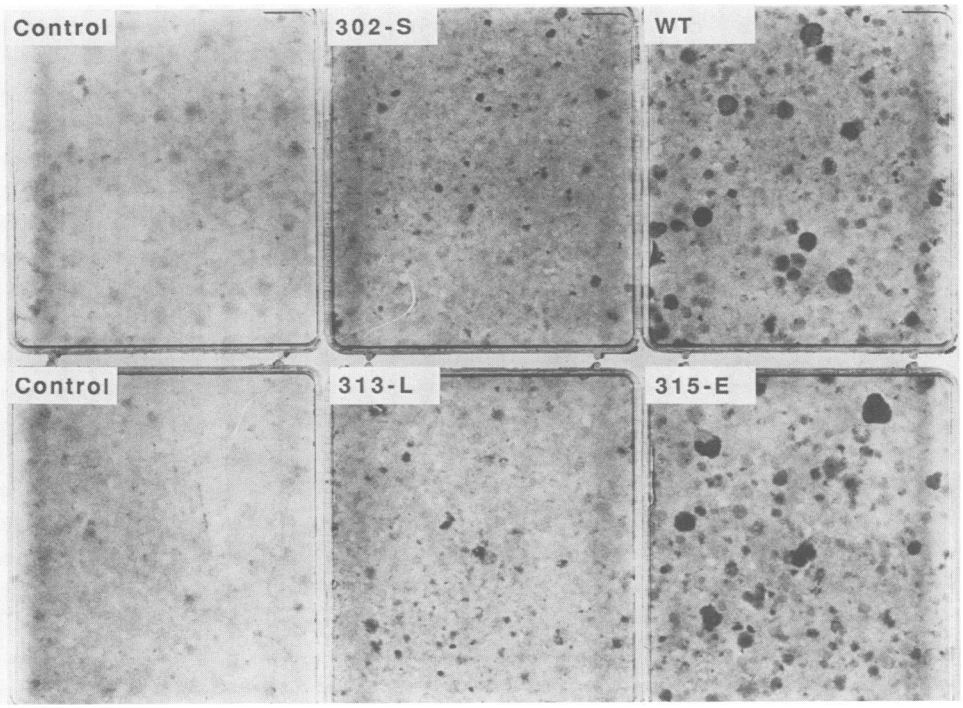

FIG. 4. Morphology of transformed foci. Primary MEF cells were transfected with control plasmid DNA, mutant DNAs (302-S, 313-L, and 315-E), and WT DNA as described in Materials and Methods. After incubation for 25 days at 37°C, the cells were fixed with methanol and stained. The appearance of the foci induced by mutants 305-S, 313-R, 317-Q, and 320-L was identical with the appearance of foci induced by mutants 302-S and 313-L (data not shown).

induced by this second class of transformation mutants could be expanded to cell lines. In contrast, more than 90% of WT foci produced cell lines under identical conditions (data not shown). Our findings suggest that mutations in the cysteine and histidine residues in the finger region reduce the immortalization capacity of T antigen. Additional defects in transformation cannot be excluded.

DISCUSSION

The mutational analysis of the presumptive zinc-binding site showed that the amino acids of the zinc finger region of SV40 large T antigen can be divided into three distinct classes. Mutants within each class have a characteristic phenotype in productive and transforming infections. Figure 5 shows the locations of these functional classes of amino acids in the putative zinc finger and summarizes their properties.

The first class consists of amino acids in the two minor loops and in the amino-terminal part of the major loop (Fig. 5, open areas). Mutations in this region have no effect on the functions of the protein. It is remarkable that an exchange of the proline at the tip of the proposed finger at position 311 has no effect on the viability of the mutant. The proline at this position is conserved among the primate polyomaviruses. Furthermore, a computer-generated structural model of T antigen (13) predicts a turn induced by the proline. Since mutations in these amino acids do not affect the WT phenotype, they may have a relatively simple structural function. However, we cannot exclude significant effects caused by amino acid substitutions different from the ones constructed or by mutations at more than one of these sites.

The second class of amino acids is clustered at the carboxy terminus of the major loop of the finger (Fig. 5,

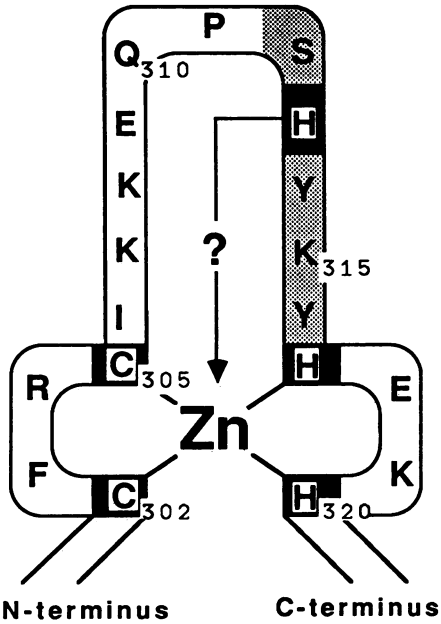

FIG. 5. Functional domains of the zinc finger of SV40 T antigen. The amino acids of the zinc finger region (positions 302 through 320) are shown in the single-letter code. The putative zinc-binding amino acids are the cysteines at positions 302 and 305 and the histidines at positions 317, 320, and possibly 313. A possible active site for DNA replication spans amino acids 312 through 316. Open areas indicate mutants with a wild-type phenotype, shaded areas indicate mutants that replicated poorly but transformed normally (a possible active site), and solid areas indicate mutants that failed to replicate and transformed poorly (possible zinc binding).

shaded areas). Mutations at these positions affect viral replication to different degrees. In vivo replication experiments showed that the defect in the mutants is related to a function in DNA replication. The clustering of these mutations suggests that this region might be an active site for a specific function in DNA replication. The replication function is not required for the transformation ability of the protein; mutant 315-E, which replicates only to a very reduced degree, has the same transformation capacity as WT SV40. The fact that the lysine at position 315 can be replaced by arginine without any effect shows that the reduction in the growth of 315-E probably results from a charge effect. The overall structure of this mutant protein must be intact because it not only has WT transforming efficiency but also binds to origin DNA as well as WT protein does (manuscript in preparation). It is not clear from our results whether the histidine at position 313 belongs to the second class of amino acids. Although the phenotype of a mutant with a mutation at this position is more characteristic of mutants in the third class, the histidine is located near the center of the putative active site.

The third class of amino acids was identified by a distinctive phenotype caused by mutations at positions 302, 305, 313, 317, and 320. Mutants with single substitutions at these positions fail to replicate at all and have a reduced ability to transform primary MEF cells. In a recent paper, Arthur et al. (1) reported that a mutant T antigen expressed in *E. coli* with the same substitutions as 302-S and 305-S failed to bind specifically to the origin of DNA replication. Since these mutations in the zinc finger are located outside the domain required for minimal specific binding (44), the effect on DNA binding is probably due to major structural alterations of the overall protein conformation. Such a change in conformation could affect multiple independent functions, including origin binding, transformation, and the function of the active site element of the zinc finger in replication. It is interesting that a conservative alteration of the histidine to the highly similar arginine at position 313 causes the same kind of phenotypic effects as do alterations of the cysteines or histidines in the positions of putative zinc ligands in a conventional zinc finger motif. This finding suggests that this histidine is also involved in the structural framework of the protein and may also interact in some way with a zinc ion. In the case of carboxypeptidase A, a histidine in the active center of the enzyme may bind zinc as a metastable intermediate with four other ligands. Christianson et al. (7) have postulated that a switch in the binding of these ligands may be important to the catalytic reaction. Similarly, the histidine at position 313 of T antigen may have a dual function. It may both bind zinc and participate in the replication function of class 2 amino acids. Studies of zinc binding by the cysteine and histidine residues of the finger region of T antigen are in progress.

ACKNOWLEDGMENTS

This investigation was supported by Public Health Service grants CA-18808, CA-38146, and 5-T32 CA-09176 awarded by the National Cancer Institute and by a postdoctoral fellowship to G.L. from the Deutsche Forschungsgemeinschaft.

LITERATURE CITED

1. **Arthur, A. K., A. Höss, and E. Fanning.** 1988. Expression of simian virus 40 T antigen in *Escherichia coli*: localization of T-antigen origin DNA-binding domain to within 129 amino acids. J. Virol. **62**:1999–2006.
2. **Berg, J. M.** 1987. Metal ions in proteins: structural and functional roles. Cold Spring Harbor Symp. Quant. Biol. **52**:579–585.
3. **Bradley, M. K., T. F. Smith, R. H. Lathrop, D. M. Livingston, and T. A. Webster.** 1987. Consensus topography in the ATP binding site of the simian virus 40 and polyomavirus large tumor antigens. Proc. Natl. Acad. Sci. USA **84**:4026–4030.
4. **Brady, J., J. B. Bolen, M. F. Radonovich, N. Salzman, and G. Khoury.** 1984. Stimulation of simian virus 40 late gene expression by simian virus 40 large tumor antigen. Proc. Natl. Acad. Sci. USA **81**:2040–2044.
5. **Chou, J. Y., and R. G. Martin.** 1975. DNA infectivity and the induction of host DNA synthesis with temperature-sensitive mutants of simian virus 40. J. Virol. **15**:145–150.
6. **Chowdhury, K., U. Deutsch, and P. Gruss.** 1987. A multigene family encoding several "finger" structures is present and differentially active in mammalian genomes. Cell **48**:771–778.
7. **Christianson, D. W., P. R. David, and W. N. Lipscomb.** 1987. Mechanism of carboxypeptidase A: hydration of a ketonic substrate analogue. Proc. Natl. Acad. Sci. USA **84**:1512–1515.
8. **Cowan, K., P. Tegtmeyer, and D. D. Anthony.** 1973. Relationship of replication and transcription of simian virus 40. Proc. Natl. Acad. Sci. USA **70**:1927–1930.
9. **Dayhoff, M. O.** 1969. Atlas of protein sequence and structure. National Biomedical Research Foundation, Silver Spring, Md.
10. **Dean, F. B., P. Bullock, Y. Murakami, R. Wobbe, L. Weissbach, and J. Hurwitz.** 1987. Simian virus 40 (SV40) DNA replication: SV40 large T antigen unwinds DNA containing the SV40 origin of replication. Proc. Natl. Acad. Sci. USA **84**:16–20.
11. **DeLucia, A. L., S. Deb, K. Partin, and P. Tegtmeyer.** 1986. Functional interactions of the simian virus 40 core origin of replication with flanking regulatory sequences. J. Virol. **57**:138–144.
12. **DeLucia, A. L., B. A. Lewton, R. Tjian, and P. Tegtmeyer.** 1983. Topography of simian virus 40 A protein-DNA complexes: arrangement of pentanucleotide interaction sites at the origin of replication. J. Virol. **46**:143–150.
13. **DePamphilis, M. L., and M. K. Bradley.** 1986. Replication of SV 40 and polyoma virus chromosomes, p. 100–246. *In* N. Salzman (ed.), The papoviridae. Plenum Publishing Corp., New York.
14. **Duncan, B. K., and B. Weiss.** 1982. Specific mutator effects of *ung* (uracil-DNA glycosylase) mutations in *Escherichia coli*. J. Bacteriol. **151**:750–755.
15. **Frankel, A. D., and C. O. Pabo.** 1988. Fingering too many proteins. Cell **53**:675.
16. **Frisque, R. J., G. L. Bream, and M. T. Cannella.** 1984. Human polyomavirus JC virus genome. J. Virol. **51**:458–469.
17. **Gannon, J. V., and D. P. Lane.** 1987. p53 and DNA polymerase α compete for binding to SV40 T antigen. Nature (London) **329**: 456–458.
18. **Giedroc, D. P., K. P. Keating, K. R. Williams, W. H. Konigsberg, and J. E. Coleman.** 1986. Gene 32 protein, the single stranded DNA binding protein from bacteriophage T4, is a zinc metalloprotein. Proc. Natl. Acad. Sci. USA **83**:8452–8456.
19. **Gluzman, Y.** 1981. SV40-transformed simian cells support the replication of early SV40 mutants. Cell **23**:175–182.
20. **Graham, F. L., and A. J. van der Eb.** 1973. A new technique for the assay of infectivity of human adenovirus 5 DNA. Virology **52**:456–467.
21. **Hirt, B.** 1967. Selective extraction of polyoma DNA from infected mouse cell cultures. J. Mol. Biol. **26**:365–369.
22. **Kadonaga, J. T., K. R. Carner, F. R. Masiarz, and R. Tjian.** 1987. Isolation of a cDNA encoding transcription factor Sp1 and functional analysis of the DNA binding domain. Cell **51**:1079–1090.
23. **Kalderon, D., and A. E. Smith.** 1984. In vitro mutagenesis of a putative DNA binding domain of SV40 large T. Virology **139**: 109–137.
24. **Khandjian, E. W., J.-M. Matter, N. Leonard, and R. Weil.** 1980. Simian virus 40 and polyoma virus stimulate overall cellular RNA and protein synthesis. Proc. Natl. Acad. Sci. USA **77**: 1476–1481.
25. **Klug, A., and D. Rhodes.** 1987. "Zinc fingers": a novel protein motif for nucleic acid recognition. Trends Biochem. Sci. **12**:464–469.

26. **Kunkel, T. A.** 1985. Rapid and efficient site-specific mutagenesis without phenotypic selection. Proc. Natl. Acad. Sci. USA **82:** 488–492.
27. **Lane, D. P., and L. V. Crawford.** 1979. T antigen is bound to a host protein in SV40-transformed cells. Nature (London) **278:** 261–263.
28. **Lillie, J. W., P. M. Loewenstein, M. R. Green, and M. Green.** 1987. Functional domains of adenovirus type 5 E1a proteins. Cell **50:**1091–1100.
29. **McCutchan, J. H., and J. S. Pagano.** 1968. Enhancement of the infectivity of simian virus 40 deoxyribonucleic acid with diethylaminoethyldextran. J. Natl. Cancer Inst. **41:**351–357.
30. **Messing, J.** 1983. New M13 vectors for cloning. Methods Enzymol. **101:**20–79.
31. **Miller, J., A. D. McLachlan, and A. Klug.** 1985. Repetitive zinc binding domains in the protein transcription factor IIIA from Xenopus oocytes. EMBO J. **4:**1609–1614.
32. **Paucha, E., D. Kalderon, R. W. Harvey, and A. E. Smith.** 1986. Simian virus 40 origin DNA-binding domain on large T antigen. J. Virol. **57:**50–64.
33. **Pawlita, M., A. Clad, and H. zur Hausen.** 1985. Complete DNA sequence of lymphotropic papovavirus: prototype of a new species of the polyomavirus genus. Virology **143:**196–211.
34. **Reed, S. I., G. R. Stark, and J. C. Alwine.** 1976. Autoregulation of simian virus 40 gene A by T antigen. Proc. Natl. Acad. Sci. USA **73:**3083–3087.
35. **Rosenberg, U. B., C. Schroeder, A. Preiss, A. Kienlin, S. Cote, I. Riede, and H. Jaeckle.** 1986. Structural homology of the product of the Drosophila Krueppel gene with Xenopus transcription factor IIIA. Nature (London) **319:**336–339.
36. **Schiff, L. S., M. L. Nibert, M. S. Co, E. G. Brown, and B. N. Fields.** 1988. Distinct binding sites for zinc and double-stranded RNA in the reovirus outer capsid protein sigma 3. Mol. Cell. Biol. **8:**273–283.
37. **Schmieg, F. I., and D. Simmons.** 1988. Characterization of the in vitro interaction between SV40 T antigen and p53: mapping of the p53 binding site. Virology **164:**132–140.
38. **Schneider, J., and E. Fanning.** 1988. Mutations in the phosphorylation sites of simian virus 40 (SV40) T antigen alter its origin DNA-binding specificity for sites I or II and affect SV40 DNA replication activity. J. Virol. **62:**1598–1605.
39. **Simmons, D. T.** 1986. DNA-binding region of the simian virus 40 tumor antigen. J. Virol. **57:**776–785.
40. **Smale, S. T., and R. Tjian.** 1986. T-antigen-DNA polymerase α complex implicated in simian virus 40 DNA replication. Mol. Cell. Biol. **6:**4077–4087.
41. **Staden, R.** 1982. An interactive graphics program for comparing and aligning nucleic acid and amino acid sequences. Nucleic Acids Res. **10:**2951–2961.
42. **Stahl, H., P. Droege, and R. Knippers.** 1986. DNA helicase activity of SV40 large tumor antigen. EMBO J. **5:**1939–1944.
43. **Stahl, H., and R. Knippers.** 1983. Simian virus 40 large tumor antigen on replicating viral chromatin: tight binding and localization on the viral genome. J. Virol. **47:**65–76.
44. **Strauss, M., P. Argani, I. J. Mohr, and Y. Gluzman.** 1987. Studies on the origin-specific DNA-binding domain of simian virus 40 large T antigen. J. Virol. **61:**3326–3330.
45. **Tegtmeyer, P.** 1972. Simian virus 40 deoxyribonucleic acid synthesis: the viral replication. J. Virol. **10:**591–598.
46. **Tegtmeyer, P., M. Schwartz, J. K. Collins, and K. Rundell.** 1975. Regulation of tumor antigen synthesis by simian virus 40 gene *A*. J. Virol. **16:**168–178.
47. **Tevethia, M. J.** 1984. Immortalization of primary mouse embryo fibroblasts with SV40 virions, viral DNA, and a subgenomic DNA fragment in a quantitative assay. Virology **137:**414–421.
48. **Tjian, R.** 1978. The binding site on SV40 DNA for a T antigen-related protein. Cell **13:**165–179.
49. **Tjian, R., and A. Robbins.** 1979. Enzymatic activities associated with a purified SV40 T-antigen related protein. Proc. Natl. Acad. Sci. USA **76:**610–614.
50. **Tooze, J. (ed.).** 1981. DNA tumor viruses: the molecular biology of tumor viruses, 2nd ed. Cold Spring Harbor Laboratory, Cold Spring Harbor, N.Y.
51. **Wiekowski, M., P. Dröge, and H. Stahl.** 1987. Monoclonal antibodies as probes for a function of large T antigen during the elongation process of simian virus 40 DNA replication. J. Virol. **61:**411–418.
52. **Wold, M. S., J. J. Li, and T. J. Kelly.** 1987. Initiation of simian virus 40 DNA replication in vitro: large-tumor-antigen and origin-dependent unwinding of the template. Proc. Natl. Acad. Sci. USA **84:**3643–3647.